

# Thermodynamic Scaling of Diffusion in Supercooled Lennard-Jones Liquids

D. Coslovich<sup>1,2</sup> and C. M. Roland<sup>3</sup>

<sup>1</sup>*Dipartimento di Fisica Teorica, Università di Trieste – Strada Costiera 11, 34100 Trieste, Italy*

<sup>2</sup>*CNR-INFM Democritos National Simulation Center – Via Beirut 2-4, 34014 Trieste, Italy*

<sup>3</sup>*Naval Research Laboratory, Code 6120, Washington, DC 20375-5342, USA*

(Dated: February 1, 2008)

The manner in which the intermolecular potential  $u(r)$  governs structural relaxation in liquids is a long standing problem in condensed matter physics. Herein we show that diffusion coefficients for simulated Lennard-Jones  $m$ -6 liquids ( $8 \leq m \leq 36$ ) in normal and moderately supercooled states are a unique function of the variable  $\rho^\gamma/T$ , where  $\rho$  is density and  $T$  is temperature. The scaling exponent  $\gamma$  is a material specific constant whose magnitude is related to the steepness of the repulsive part of  $u(r)$ , evaluated around the distance of closest approach between particles probed in the supercooled regime. Approximations of  $u(r)$  in terms of inverse power laws are also discussed.

PACS numbers: 61.43.Fs, 61.20.Lc, 64.70.Pf, 61.20.Ja

Establishing a quantitative connection between the relaxation properties of a liquid and the interactions among its constituent molecules is the *sine qua non* for fundamental understanding and prediction of the dynamical properties. The supercooled regime is of particular interest, since both intermolecular forces and steric constraints (excluded volume) exert significant effects on the dynamics. This makes temperature, pressure, and volume essential experimental variables to characterize the relaxation properties. One successful approach to at least categorize dynamic properties of supercooled liquids and polymers is by expressing them as a function of the ratio of mass density,  $\rho$ , to temperature,  $T$ , with the former raised to a material specific constant  $\gamma$ , *viz.*

$$x = \mathfrak{F}(\rho^\gamma/T) \quad (1)$$

where  $x$  is the dynamic quantity under consideration, such as the structural relaxation time  $\tau$ , the viscosity  $\eta$ , or the diffusion coefficient  $D$ , and  $\mathfrak{F}$  is a function. This scaling was first applied to a Lennard-Jones (LJ) fluid, with  $\gamma = 4$  yielding approximate master curves of the reduced “excess” viscosity for different thermodynamic conditions [1]. More recently Eq. (1) has been shown to superpose relaxation times measured by neutron scattering [2], light scattering [3], viscosity [4], and dielectric spectroscopy [5, 6, 7, 8, 9] for a broad range of materials, including polymer blends and ionic liquids. The scaling exponent  $\gamma$ , which varies in the range from 0.13 to 8.5 [10], is a measure of the contribution of density (or volume) to the dynamics, relative to that due to temperature. The only breakdown of the scaling is observed for hydrogen-bonded liquids, in which the concentration of H-bonds changes with  $T$  and  $P$ , causing  $\tau$  to deviate from Eq. (1) [4].

The function  $\mathfrak{F}$  in Eq. (1) is unknown *a priori*. Its form can be derived from entropy models for the glass transition, leading to an exponential dependence of  $\log \tau$  on  $\rho^\gamma/T$  [11, 12]. Another interpretation of the scaling is that the supercooled dynamics is governed by activated

processes with an effective activation energy  $E(\rho, T)$  [13], in which the  $\rho$ -dependence of  $E(\rho, T)$  can be factored and expressed in terms of a power law of  $\rho$ . The power law scaling arose from the idea that the intermolecular potential for liquids can be approximated as a repulsive inverse power law (IPL), with the weaker attractive forces treated as a spatially-uniform background term [14, 15, 16]

$$u(r) \sim r^{-\overline{m}} + \text{const} \quad (2)$$

where  $r$  is the intermolecular distance. In the case of an IPL, in fact, all *reduced* dynamical quantities [17] can be cast in the form of Eq. (1) with  $\gamma = \overline{m}/3$ , i.e., the thermodynamic scaling is strictly obeyed. For instance, this applies to the reduced diffusion coefficient  $D^* \sim (\rho^{1/3} T^{-1/2}) D \sim (T^{3/\overline{m}-1/2}) D$ . A similar reduction of  $D$  by macroscopic variables ( $\rho$  and  $T$ ) has also been employed in entropy scaling laws of diffusion [18].

The IPL approximation emphasizes the dominant role of the short-range repulsive interactions for local properties such as structural relaxation. Various groups have explored through numerical simulations the relationship of the steepness of the repulsive potential to properties such as the equation of state [19, 20, 21], longitudinal wave transmission [22], vibrational spectrum [23], liquid [24] and gaseous [25] transport, the correlation between fluctuations of energy and pressure [26], and the fragility [27, 28]. Recently two simulations have appeared in which Eq. (1) was used to superpose dynamical data for polymer chains described using an LJ  $m$ -6 potential with  $m = 12$  and an added term for the intrachain interactions. The results appear contradictory: Tsolou et al. [29] obtained a scaling exponent of  $\gamma = 2.8$  for the segmental relaxation times of simulated 1,4-polybutadiene, while Budzien et al. [30] superposed diffusion coefficients for prototypical polymer chains using  $\gamma = 6$  when attraction were included in the simulation and  $\gamma = 12$  when they were omitted. Thus, the scaling exponent  $\gamma$  is either less than [29] or greater than [30]  $m/3$ .

To clarify this situation and to establish a connection between the thermodynamic scaling and the repulsive part of the intermolecular potential, we carried out molecular dynamics simulations for supercooled LJ  $m$ - $n$  liquids, in which the repulsive exponent  $m$  was systematically varied. Our models are binary mixtures composed of  $N = 500$  particles enclosed in a cubic box with periodic boundary conditions and interacting with a LJ  $m$ - $n$  potential

$$u_{\alpha\beta}(r) = 4\epsilon_{\alpha\beta} [(\sigma_{\alpha\beta}/r)^m - (\sigma_{\alpha\beta}/r)^n] \quad (3)$$

where  $\alpha, \beta = 1, 2$  are indexes of species. We fixed the attractive exponent  $n = 6$ , as in the standard LJ potential, and varied  $m = 8, 12, 24, 36$ . The potential  $u_{\alpha\beta}(r)$  was smoothed at  $r_c = 2.5\sigma_{\alpha\beta}$  using the cutoff scheme of Stoddard and Ford [31]. Reduced LJ units are used, assuming  $\sigma_{11}$ ,  $\epsilon_{11}$  and  $\sqrt{m_1\sigma_{11}^2/\epsilon_{11}}$  as units of distance, energy and time respectively. The mixture on which we focus is an additive, equimolar mixture with size ratio  $\lambda = \sigma_{22}/\sigma_{11} = 0.64$ , equal masses  $m_1 = m_2 = 1.0$  and a unique energy scale  $\epsilon_{\alpha\beta} = 1.0$ . The choice  $m = 12$  corresponds to the AMLJ-0.64 mixture studied in [32, 33]. The samples were quenched isobarically at different pressures  $P = 5, 10, 20$  by coupling the system to Berendsen thermostat and barostat during equilibration (see [32] for details), and performing the production runs in the NVE ensemble using the Velocity-Verlet algorithm. The timestep  $\delta t$  was varied according to the repulsive exponent, ranging from 0.001 ( $m = 36$ ) to 0.004 ( $m = 8$ ) at high  $T$ , and from 0.003 ( $m = 36$ ) to 0.008 ( $m = 8$ ) at low  $T$ . The equilibration criteria were similar to the ones used in [32].

The effectiveness of the thermodynamic scaling for LJ  $m$ -6 systems is demonstrated in Fig. 1 for different values of the repulsive exponent  $m$ . For each  $m$ , reduced diffusion coefficients  $D^* = (\rho^{1/3}T^{-1/2})D$  were gathered along different isobaric paths ( $P = 5, 10, 20$ ) and the material specific scaling exponent  $\gamma$  was obtained by maximizing the overlap between different sets of data, plotted as a function of  $\rho^\gamma/T$ . Repeating the analysis for  $D$ , instead of  $D^*$ , yields very similar values of  $\gamma$ , but the quality of the scaling for  $D^*$  is slightly superior. Our data span roughly 5 decades of variation of  $D$ , over about two of which the temperature is lower than the so-called onset temperature  $T_O$  [34], where non-exponential relaxation typical of the supercooled regime first becomes apparent upon cooling the liquid. Analyzing the variation of the scaling exponent in our models, we find that  $\gamma$  increases with increasing  $m$ , but its actual value is systematically larger than  $m/3$ . For instance, in the case  $m = 12$  we obtain  $\gamma = 5.0$ , a value which we also found to provide scaling of  $D^*$  for other supercooled Lennard-Jones ( $m = 12$ ) mixtures, such as the AMLJ-0.76 mixture introduced in [32] and the mixture of Kob and Andersen [35].

The origin of the discrepancy between  $\gamma$  and  $m/3$  lies in the fact that the asymptotic region of small interpar-

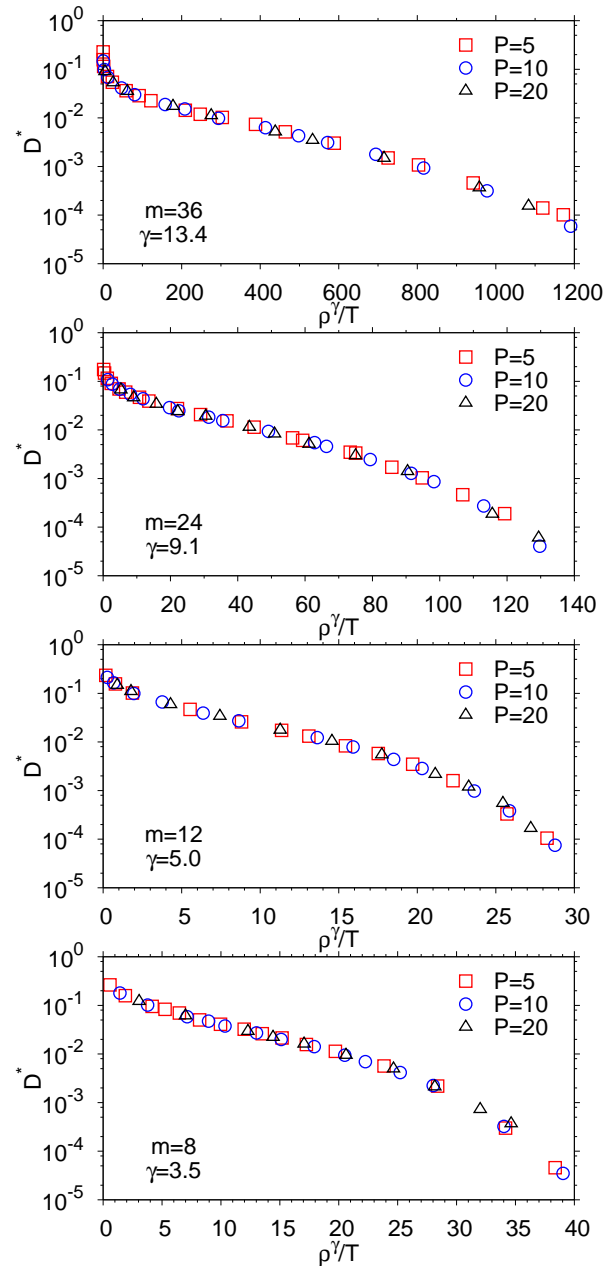


FIG. 1: (color online). Reduced diffusion coefficients  $D^*$  as a function of  $\rho^\gamma/T$  for different values of the repulsive exponent  $m$  at different pressures:  $P = 5$  (squares),  $P = 10$  (circles), and  $P = 20$  (triangles). From top to bottom:  $m = 36$  ( $\gamma = 13.4$ ),  $m = 24$  ( $\gamma = 9.1$ ),  $m = 12$  ( $\gamma = 5.0$ ), and  $m = 8$  ( $\gamma = 3.5$ ). The estimated uncertainty on  $\gamma$  is  $\pm 0.1$  ( $\pm 0.2$  for  $m = 36$ ).

ticle distances, in which  $u(r) \sim r^{-m}$ , is not dynamically accessible in normal simulation conditions. The presence of the fixed attractive term in the potential (Eq. (3)) gives rise to an effective IPL which is steeper in the region of  $r$  close to the minimum than in the  $r \rightarrow 0$  limit. This effect is illustrated in Fig. 2 for the case  $m = 24$ . The lower panel of Fig. 2 shows a fit of the pair potential  $u_{11}(r)$  to an IPL (Eq. (2)) performed in the range

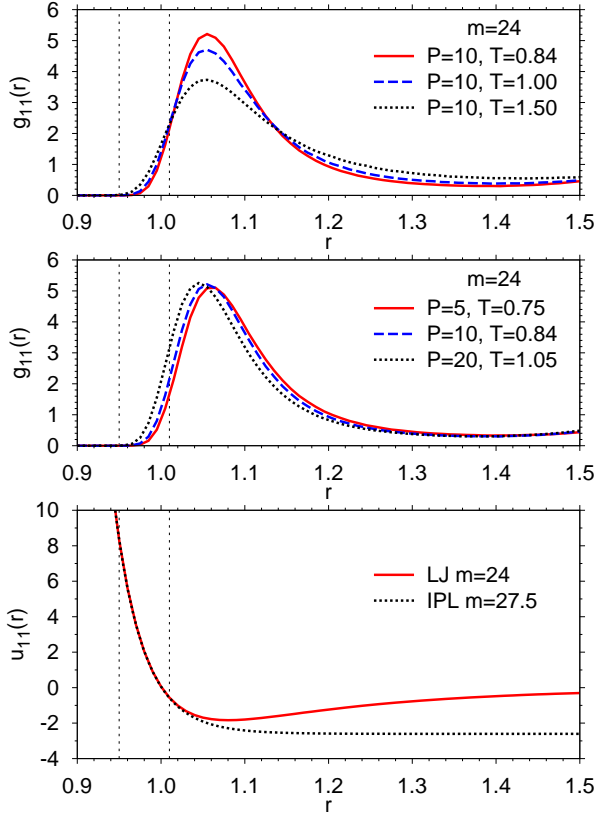


FIG. 2: (color online). Top panel: radial distribution functions between large particles  $g_{11}(r)$  at  $P = 10$  for  $T \lesssim T_O$ :  $T = 1.20$  (dotted),  $T = 1.00$  (dashed), and  $T = 0.84$  (solid). Middle panel:  $g_{11}(r)$  at the lowest equilibrated  $T$ :  $T = 0.75$  at  $P = 5$  (dotted),  $T = 0.84$  at  $P = 10$  (dashed), and  $T = 1.05$  at  $P = 20$  (solid). Bottom panel: pair potential  $u_{11}(r)$  (solid) and fitted IPL (dotted) in the range  $[0.95 : 1.01]$ . The latter range is indicated by vertical dotted lines in all panels.

$[r_0 : r_1]$ , with  $r_0 = 0.95$  and  $r_1 = 1.01$ . The value  $\overline{m} = 27.5$  obtained through this procedure is indeed larger than  $m = 24$  and is in very good agreement with the value expected from the dynamical scaling ( $3\gamma = 27.3 \pm 0.03$ ). The range  $[r_0 : r_1]$  corresponds to typical distances of closest approach between particles probed within our simulation conditions, as it can be seen by inspection of the radial distribution functions  $g_{11}(r)$  (see upper panels of Fig. 2). Extending the range for the fit up to  $r_1 = 1.06$ , which is close to the average position of the first peak in the  $g_{11}(r)$ , yields a larger value  $\overline{m} = 28.8$ , revealing how  $\gamma$  is dictated by the portion of  $r$  around the distance of closest approach in the supercooled regime.

To proceed in a more systematic way, we considered all  $\alpha - \beta$  pairs (1-1, 1-2 and 2-2) in the potential  $u_{\alpha\beta}(r)$  and performed a simultaneous fit to the following IPL

$$\overline{u}_{\alpha\beta}(r) = \overline{\epsilon}(\sigma_{\alpha\beta}/r)^{\overline{m}} + \overline{k}. \quad (4)$$

The range for fitting was defined by two conventional distances determined from the radial distribution func-

TABLE I: Parameters of IPL approximations for  $u_{\alpha\beta}(r)$ . The effective exponent  $\overline{m}$  is obtained from fitting to Eq. (4), whereas  $\overline{\epsilon}$ ,  $\overline{k}$ , and  $\overline{\sigma}$  are the optimal values for Eq. (5).

$m$	$3\gamma$	$\overline{m}$	$\overline{\sigma}$	$\overline{\epsilon}$	$\overline{k}$
8	10.5(3)	10.9	0.86	0.93	-1.05
12	15.0(3)	14.9	0.93	1.74	-1.80
24	27.3(3)	27.2	0.97	2.72	-2.74
36	40.2(6)	39.9	0.99	3.01	-3.01

tions  $g_{\alpha\beta}(r)$ : the distance of closest approach between particles,  $r_0$ , (i.e., the value of  $r$  for which the  $g_{\alpha\beta}(r)$  first becomes non-zero) and the position corresponding to half of the height of the first peak,  $r_1$ , (i.e.,  $g_{\alpha\beta}(r_1) = g_{\alpha\beta}(r_m)/2$  where  $r_m$  is the position of the first peak and  $r_0 < r_1 < r_m$ ). These quantities depend on the thermodynamic state under consideration, but their variation with  $P$  and  $T$  is mild within our simulation conditions [38]. Our interest being the supercooled regime, we simply consider the interval  $[r_0 : r_1]$  obtained from the low- $T$  behavior of the  $g_{\alpha\beta}(r)$ . For each  $\alpha - \beta$  pair we used the corresponding range  $[r_0 : r_1]$  for fitting. In general, the fitted values of  $\overline{m}$  are in good agreement with  $3\gamma$  (see Table I) for all values of  $m$ . Thus, the scaling exponent can be reasonably accounted for in terms of an IPL approximation of the pair potential, provided that a sensible choice of the relevant range of distances is made.

The above procedure suggests that a model of soft-spheres (SS) with  $\overline{m} = 3\gamma$  should provide a good reference system for the LJ  $m$ -6 mixtures. To this aim, we approximate Eq. (3) with

$$v_{\alpha\beta}(r) = \begin{cases} \overline{\epsilon}(\sigma_{\alpha\beta}/r)^{\overline{m}} + \overline{k} & r < \overline{\sigma}\sigma_{\alpha\beta} \\ u_{\alpha\beta}(r) & r \geq \overline{\sigma}\sigma_{\alpha\beta} \end{cases} \quad (5)$$

where  $\overline{m}$ ,  $\overline{\epsilon}$ , and  $\overline{k}$  are expressed in terms of  $\overline{\sigma}$  by requiring continuity of 0th, 1th, and 2th derivatives of  $v_{\alpha\beta}(r)$  at  $r = \overline{\sigma}\sigma_{\alpha\beta}$ . The value of  $\overline{\sigma}$  is then fixed by requiring that  $3\gamma = \overline{m}(\overline{\sigma}) = (m^2/\overline{\sigma}^{m+1} - n^2/\overline{\sigma}^{n+1})/(m/\overline{\sigma}^{m+1} - n/\overline{\sigma}^{n+1})$ . The parameters defining the reference SS models for all values of  $m$  are reported in Table I. We checked that the distance  $\overline{\sigma}\sigma_{\alpha\beta}$  always lies in the range  $[r_0 : r_1]$  defined above. Diffusivity data for the LJ 12-6 mixture are compared in Fig. 3 to those of the corresponding reference SS mixture along two isochores ( $\rho = 1.5$ ,  $\rho = 1.7$ ), which correspond to typical densities attained at low  $T$  by the LJ system (at constant  $P$ ). The trend of  $D(T)$  for the reference system closely follows the one for the full LJ system. As expected, the SS mixture has a larger diffusion coefficient for a given thermodynamic state. The contribution to  $D$  due to the attractive part of the potential could also be explicitly included using a WCA-like splitting of  $v_{\alpha\beta}(r)$  [36]. For the present purposes, however, it is more useful to note that a simple rescaling of

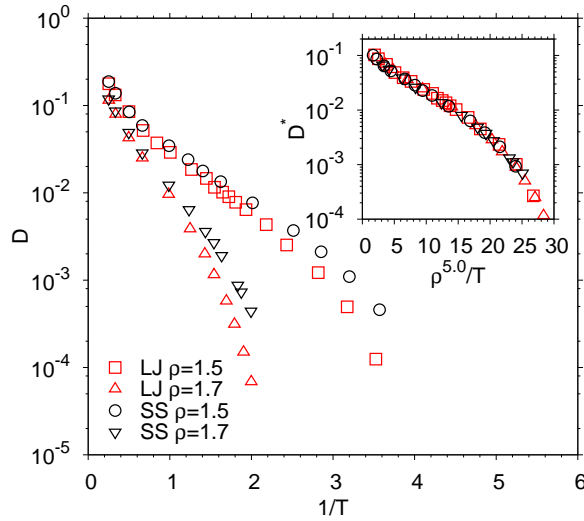


FIG. 3: (color online). Arrhenius plot of diffusion coefficient  $D$  for the LJ 12-6 mixture and the reference SS mixture ( $\bar{m} = 15.0$ ,  $\bar{\epsilon} = 1.74$ ) along two isochores:  $\rho = 1.5$  and  $\rho = 1.7$ . Inset: reduced diffusion coefficient  $D^*$  as a function of  $\rho^{5.0}/T$ . For the SS mixture a reoptimized energy scale  $\bar{\epsilon} = 1.13\bar{\epsilon}$  was used.

$\bar{\epsilon}$  (increased by around 10%) yields an excellent superposition of  $D^*$  for all sets of data (see inset of Fig. 3). Thus, at least to a first approximation, the contribution of the attractive part of the potential to the dynamics alters the shape of the function  $\mathfrak{F}$  *without affecting* the scaling exponent  $\gamma$ .

To summarize, the thermodynamic scaling of the diffusion coefficient in supercooled LJ  $m$ -6 mixtures reflects the importance of the repulsive part of the pair potential in determining the dynamical properties of these systems. The scaling exponent  $\gamma$  is larger than  $m/3$  for LJ  $m$ -6 liquids, a fact which can be rationalized by approximating the repulsive part of the potential with an IPL having exponent  $\bar{m} \approx 3\gamma$ . Generalizing such arguments to more realistic models of glass-formers [29, 30] and establishing connections with other scaling procedures for  $D^*$  [18, 37] are open challenges for future investigations.

We thank G. Pastore and J. Dyre for useful discussions. Computational resources were obtained through a grant within the agreement between the University of Trieste and CINECA (Italy). The work at NRL was supported by the Office of Naval Research.

---

[1] W. T. Ashurst and W. G. Hoover, Phys. Rev. A **11**, 658 (1975).  
[2] A. Tölle, Rep. Prog. Phys. **64**, 1473 (2001).  
[3] C. Dreyfus, A. Le Grand, J. Gapinski, W. Steffen, and A. Patkowski, Eur. J. Phys. **42**, 309 (2004).  
[4] C. M. Roland, S. Bair, and R. Casalini, J. Chem. Phys. **125**, 124508 (2006).

[5] R. Casalini and C. M. Roland, Phys. Rev. E **69**, 062501 (2004).  
[6] C. Alba-Simionesco, A. Cailliaux, A. Alegria, and G. Tarjus, Europhys. Lett. **68**, 58 (2004).  
[7] S. Urban and A. Würflinger, Phys. Rev. E **72**, 021707 (2005).  
[8] A. Reiser, G. Kasper, and S. Hunklinger, Phys. Rev. B **72**, 094204 (2005).  
[9] K. Z. Win and N. Menon, Phys. Rev. E **73**, 040501(R) (2006).  
[10] C. M. Roland, S. Hensel-Bielowka, M. Paluch, and R. Casalini, Rep. Prog. Phys. **68**, 1405 (2005).  
[11] R. Casalini, U. Mohanty, and C. M. Roland, J. Chem. Phys. **125**, 014505 (2006).  
[12] R. Casalini and C. M. Roland, J. Non-Cryst. Solids (to be published), cond-mat/0703518.  
[13] G. Tarjus, D. Kivelson, S. Mossa, and C. Alba-Simionesco, J. Chem. Phys. **120**, 6135 (2004).  
[14] W. G. Hoover and M. Ross, Contemp. Phys. **12**, 339 (1971).  
[15] D. Chandler, J. D. Weeks, and H. C. Andersen, Science **220**, 787 (1983).  
[16] J. P. Hansen and I. R. McDonald, *Theory of Simple Liquids* (Academic Press, London, 1986), 2nd ed.  
[17] Y. Hiwatari, H. Matsuda, T. Ogawa, N. Ogita, and A. Ueda, Progr. Theor. Phys. **52**, 1105 (1974).  
[18] Y. Rosenfeld, J. Phys.: Condens. Matter **11**, 5415 (1999).  
[19] T. Lafitte, D. Bessieres, M. Pineiro, and J. Daridon, J. Chem. Phys. **124**, 024509 (2006).  
[20] D. M. Heyes and A. C. Branka, J. Chem. Phys. **122**, 234504 (2005).  
[21] I. I. Adamenko, A. N. Grigoriev, and Y. I. Kuzokov, J. Mol. Liq. **105**, 261 (2003).  
[22] N. Anento, J. A. Padro, and M. Canales, J. Chem. Phys. **111**, 10201 (1990).  
[23] S. Kambayashi and Y. Hiwatari, Phys. Rev. E **49**, 1251 (1994).  
[24] G. Galliero, C. Boned, A. Baylaucq, and F. Montel, Phys. Rev. E **73**, 061201 (2006).  
[25] S. Chapman and T. G. Cowling, *The Mathematical Theory of Non-Uniform Gases* (Cambridge Mathematical Library, Cambridge, 1970).  
[26] U. R. Pedersen, N. Bailey, T. B. Schröder, and J. C. Dyre (2007), cond-mat/0702146.  
[27] P. Bordat, F. Affouard, M. Descamps, and K. L. Ngai, Phys. Rev. Lett. **93**, 105502 (2004).  
[28] C. De Michele, F. Sciortino, and A. Coniglio, J. Phys.: Condens. Matter **16**, L489 (2004).  
[29] G. Tsolou, V. A. Harmandaris, and V. G. Mavrantzas, J. Chem. Phys. **124**, 084906 (2006).  
[30] J. Budzien, J. D. McCoy, and D. B. Adolf, J. Chem. Phys. **121**, 10291 (2004).  
[31] S. D. Stoddard and J. Ford, Phys. Rev. A **8**, 1504 (1973).  
[32] D. Coslovich and G. Pastore, J. Chem. Phys. (to be published), arXiv:0705.0626.  
[33] D. Coslovich and G. Pastore, J. Chem. Phys. (to be published), arXiv:0705.0629.  
[34] S. Sastry, P. G. Debenedetti, and F. H. Stillinger, Nature **393**, 554 (1998).  
[35] W. Kob and H. C. Andersen, Phys. Rev. E **51**, 4626 (1995).  
[36] J. E. Straub, Mol. Phys. **76**, 373 (1992).  
[37] M. Dzугutov, Nature (London) **381**, 137 (1996).  
[38] At fixed  $P$ ,  $r_0$  and  $r_1$  show a weak increase with decrease-

ing  $T$ , but they become almost  $T$ -independent below  $T_O$ .